CONF-9510119--40 ANL/XFD/CP--87519

LIQUID-METAL-COOLED, CURVED-CRYSTAL MONOCHROMATOR FOR ADVANCED PHOTON SOURCE BENDING-MAGNET BEAMLINE 1-BM*

S. Brauer[1], B. Rodricks[1], L. Assoufid,[1] M. Beno[2], and G. Knapp[2]

[1]Experimental Facilities Division
Advanced Photon Source, Argonne National Laboratory
Argonne, IL 60439

[2]Materials Science Division, Argonne National Laboratory
Argonne, IL 60439

RECEIVED
SEP 03 1996
OSTI

June 1996

The submitted manuscript has been authored by a contractor of the U.S. Government under contract No. W-31-109-ENG-38. Accordingly, the U.S. Government retains a nonexclusive, royalty-free license to publish or reproduce the published form of this contribution, or allow others to do so, for U.S. Government purposes.

Presented at the SRI '95 APS X-ray Centennial Symposium/Seventh Users Meeting for the APS, Argonne, IL, October 16-20, 1995; to be published in the proceedings as a peer-reviewed volume of the *Review of Scientific Instruments* in CD-ROM format.

*This work was supported by the U.S. Department of Energy, Basic Energy Sciences-Materials Sciences, under contract #W-31-109-ENG-38.

DISTRIBUTION OF THIS DOCUMENT IS UNLIMITED

MASTER

DISCLAIMER

Portions of this document may be illegible in electronic image products. Images are produced from the best available original document.

Liquid-metal-cooled curved-crystal monochromator for Advanced Photon Source bending-magnet beamline 1-BM

S. Brauer, B. Rodricks, and L. Assoufid
Experimental Facilities Division, Advanced Photon Source, Argonne National Laboratory, 9700 S. Cass Avenue, Argonne, IL 60439

M.A. Beno, and G.S. Knapp
Materials Science Division, Argonne National Laboratory, 9700 S. Cass Avenue, Argonne, IL 60439

(Presented on 19 October 1995)

We describe a horizontally focusing curved-crystal monochromator that invokes a 4-point bending scheme and a liquid-metal cooling bath. The device has been designed for dispersive diffraction and spectroscopy in the 5-20 keV range, with a predicted focal spot size of ≤100 μm. To minimize thermal distortions and thermal equilibration time, the 355 × 32 × 0.8 mm crystal will be nearly half submerged in a bath of Ga-In-Sn-Zn alloy. The liquid metal thermally couples the crystal to the water-cooled Cu frame, while permitting the required crystal bending. Calculated thermal profiles and anticipated focusing properties are discussed. © *1995 American Institute of Physics*.

I. INTRODUCTION

A curved crystal optic may be used to focus a portion of the light from a synchrotron x-ray source, and to thereby form a beam in which photon energy varies approximately linearly with angle. Such an energy dispersed beam may be used to perform absorption spectroscopy measurements, such as the various x-ray absorption fine structure (XAFS) techniques,[1-4] in addition to novel diffraction measurements including anomalous scattering,[5] diffraction anomalous fine structure (DAFS)[6] and continuous energy diffraction spectroscopy (CEDS).[7] In general, dispersive geometries benefit from the ability to employ a position sensitive detector (PSD) to collect data over a range of energies or wave vectors in parallel. These geometries are therefore particularly amenable to time-resolved studies, where it is desired to make rapid structural measurements *in situ* during structural transformations. For example, extended XAFS spectra may be obtained by focusing the energy dispersed beam on a thin specimen and using a fast linear photodiode array detector to measure the transmitted flux as a function of angle.[1-4]

A versatile monochromator for dispersive studies must provide adjustability of energy and energy bandwidth in addition to a strong correlation between angle and energy in the focused exit beam. This may be effectively achieved through the dynamic elastic bending of a flat perfect crystal. The average x-ray energy is then determined by the average Bragg angle θ_B, and the bandwidth is varied by changing the average radius of curvature of the crystal R (which also changes the focal position). When bending a flat crystal, the ideal surface figure is an elliptical section that has the source at one focus and the experiment (sample) at the other. The requirements for accuracy and stability of the figure place stringent demands on the mechanical integrity and reproducibility of the bender mechanism. At third-generation sources such as the Advanced Photon Source (APS), these challenges are exacerbated by the high power and power density on the crystal. In response, the design must provide uniform and high cooling power while still permitting fine crystal deformations. This is particularly challenging because any rigid mechanical contact with the crystal, apart from the bending points, will disrupt the figure.

We now outline the design parameters of the curved-crystal monochromator for the time-resolved station on beamline 1-BM.[8] The horizontal x-ray source size has been measured to be $A = 350 \pm 25$ μm FWHM,[9] and our goal is to obtain a horizontal focal spot size of $\Delta x \leq 100$ μm in the dispersive mode. The beamline has a source-to-crystal distance of $p =$ 32 m, and the monochromator will have a horizontal acceptance of 3.1 mrad. The uncommonly large experimental station, 1-BM-B, permits crystal-to-focus distances in the range of $q = 0.5$-4 m over a wide range of scattering angles. The energy range of most interest is 5-16 keV, which corresponds to an angular range of $2\theta = 20$-85° for a Si(220) crystal. Higher energies will be reached via higher order reflections. The total power emitted by the source is ≈90 W per horizontal milliradian at 100 mA ring current. Although a harmonic-rejection high-heat-load vertically focusing mirror will eventually be installed upstream of the bent crystal, the monochromator must perform as the first optical element during the initial phase of operations. In addition, the design must permit the use of asymmetrically cut crystals for both nondispersive and dispersion-enhanced operations. The same bender design will be implemented for high energy (60-100 keV) and Compton scattering applications at an APS wiggler beamline.

II. FOCUSING PROPERTIES

Treatments of the focusing properties of curved-crystal monochromators are available in the literature.[10-12] We will discuss only the bending of flat crystals to approximately elliptical sections, as appropriate for meridinal Bragg (reflection) geometeries. Our goal is to produce a dispersive beam that has the smallest possible focal spot and contains a broad energy bandwidth ($\Delta E/E \approx 0.1$) with a strong linear correlation between angle and energy (to provide good energy resolution).

The results for a Johansson geometry (cylindrically ground and then cylindrically bent crystal) provide a rather accurate description of the focusing properties of an elliptically bent crystal, when we employ the mean radius of curvature R. For operation at an average wavelength λ and a crystal lattice spacing d, the average Bragg angle is $\theta_B \equiv \sin^{-1}(\lambda/2d)$. We introduce the crystal miscut angle α and both the source-to-crystal and crystal-to-focus lengths p and q, respectively. The focusing condition is

$$\frac{\sin(\theta_B+\alpha)+\sin(\theta_B-\alpha)}{R} = \frac{\sin^2(\theta_B+\alpha)}{p} + \frac{\sin^2(\theta_B-\alpha)}{q}. \quad (1)$$

In the absence of aberrations, the beam size Δx, divergence $\Delta x'$ and total energy range $\Delta E/E$ at the focal spot are given by

$$\Delta x^2 = \left[\tau(1-|b|)q\right]^2 + \left[\omega_0 \frac{(1-|b|)}{\sqrt{|b|}} q\right]^2 + \left[\frac{Aq}{p}\right]^2 \quad (2)$$

$$\Delta x'^2 = \left[\tau(1-|b|)\right]^2 + \left[\omega_0 \frac{(1-|b|)}{\sqrt{|b|}}\right]^2 + \left[\frac{A}{p}\right]^2 + \left[\frac{L\sin(\theta_B-\alpha)}{q}\right]^2 \quad (3)$$

$$\left(\frac{\Delta E}{E}\right)^2 = \cot^2\theta_B \left\{\tau^2 + {\omega_0}^2 + \left[\frac{A}{p}\right]^2\right\} \quad (4)$$

where L is the illuminated length of crystal, $b=\sin(\alpha+\theta_B)/\sin(\alpha-\theta_B)$ is the asymmetry factor, ω_0 is the Darwin width for a symmetrically cut flat crystal at the energy of interest and

$$\tau = L\left(\frac{1}{R} - \frac{\sin(\theta_B+\alpha)}{p}\right) \quad (5)$$

is a parameter that vanishes at the Rowland condition. In the simplest dispersive mode, a symmetrically cut crystal is chosen (b = -1) resulting in a very linear relation between energy and angle, the slope of which is $\Delta E/\Delta x'$. In the absence of aberrations, an elliptical bend would then result in a focal spot size that is equal to the demagnification of the source Aq/p.

The energy resolution obtained in the dispersive geometry[1] is a convolution of contributions arising from (i) the source size, (ii) the spatial resolution of the detector and its distance from the focus, (iii) the angular width of diffraction from the crystal ω_0, and (iv) the penetration depth of x-rays into the crystal. We have estimated the energy resolution for the parameters at 1-BM, when a 25-mm-long detector, composed of 20-μm-wide pixels, is positioned to intercept the entire beam width downstream of the focus. Under these conditions, when a symmetric Si(220) crystal is bent to provide 10% total energy bandwidth, the estimated resolution is 0.4 eV at 5 keV and 1.6 eV at 16 keV. This resolution will be adequate to produce high quality XAFS spectra.

This focusing geometry has also been widely used for monochromatic focusing of synchrotron radiation, by selecting a crystal of appropriate asymmetry such that τ=0. Here, the beam has an energy bandpass approximately equal to that which would be obtained from the same source with a flat crystal. In that case, the angular width of the focused beam is approximately equal to the accepted incident divergence, and all angles contain approximately the same range of energies (nondispersive).

III. BENDER MECHANISM

Various strategies have been devised for bending crystals to approximate the desired elliptical figure. These include (i) triangular crystal with 3-point bend, (ii) contoured near-triangular crystal with 3-point bend, (iii) rectangular crystal, 4-point bend, and (iv) contoured near-rectangular crystal, 4-point bend. All these methods provide nearly the same energy bandpass and angle-energy correlation in the beam for the same source size, beamline geometry, and crystal size, surface orientation, and mean radius of curvature. The methods differ however in their ability to produce a small focal spot. Method (i) provides a nearly cylindrical figure and the largest aberration.[13] Method (ii) can provide a very nearly elliptical bend, although a differently contoured crystal is required to get the ideal figure at each energy.[3] Method (iii) is more versatile because it allows independent adjustment of the bending moment at each end.[14] The resulting figure is intermediate to an ellipse and a cylinder, resulting in some aberrant broadening of the focal spot. Method (iv) can in principle provide a very nearly elliptical shape and a very small focal spot size for a range of energies, though this remains to be demonstrated.[15] Also, for typical values of p and q on the 1-BM beamline, the proposed corrections to a rectangular crystal shape[15] are very small. For our application, we have selected method (iii) because a single crystal, of simple shape, should provide a sufficiently small focal spot over a wide energy range.

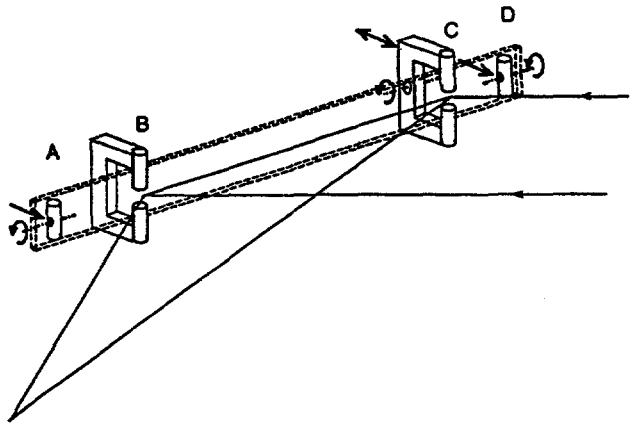

FIG. 1. Schematic representation of the 4-point bending scheme. The positions at which the crystal is constrained are labeled A, B, C, and D.

The basic bender mechanism is similar to that of DeWolff[14] and is shown in Figure 1. The crystal has dimensions 355 x 32 x 0.8 mm^3 and is sketched with dashed lines. The four bender points are labeled A, B, C and D. To

prevent blocking the beam, both bend points B and C consist of a separated pair of co-axial stainless steel rods located in front of the crystal and supported from behind by c-shaped brackets. Both A and D consist of stainless steel rods, which are pushed onto the back face of the crystal, near its ends, to apply the bending torque. While B is a rigid constraint, the rods at A, C, and D all have a rotational degree of freedom parallel to the long axis of the crystal. Thus any small twist along the long axis of the crystal (for example due to surface asperities at the interface of the crystal and the rods) can be actively removed by controlling the angular orientation of the clamp at C.

Cooling of the crystal is required to prevent excess thermal distortion of the figure and the reflecting lattice planes, as well as to minimize the time for the device to reach a thermal steady state after the beam shutter is opened. Our cooling scheme is to submerge the lower half of the crystal in a bath of Ga-In-Sn-Zn alloy, which thermally couples the crystal to the water-cooled Cu frame. The alloy was chosen because it remains liquid down to ≈8 °C. Bliss et al.[16] have used a similar technique to cool a triangular crystal. The x-ray beam will strike the crystal 3 mm above the surface of the Cu frame, and the liquid meniscus. This scheme permits the required crystal deformations, while providing nearly constant cooling along the length of the crystal. Thermal modeling of the geometry is described in the next section.

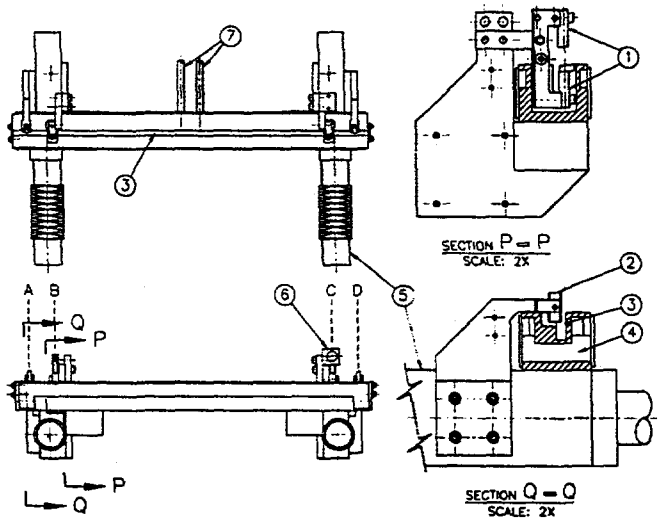

FIG. 2: Schematic of the crystal bending apparatus. The enlarged cross sections show the rods which constrain the crystal (1,2), the slot in which the crystal will be half submerged in liquid metal (3) and water-cooling channels in the copper frame (4). Also shown are the linear translation stages for controlling the crystal bend (5), the mounting bracket for the antitwist mechanism (6) and the cooling water input and output (7). (The crystal and liquid metal are not shown.)

The actual bender mechanism is illustrated in Figure 2. Cooling water flows around the Cu body through integrated cooling channels. The water input and output are the two Cu tubes protruding near the center. Stepper-motor-controlled linear translation stages are used to deform the crystal. These are located below the Cu frame, and therefore out of the scattering plane, to reduce radiation damage to the motors. The stages have 0.1-μm resolution and are being prepared with dry vacuum lubricant. In general, we have tried to minimize the amount of metal located behind the crystal in the scattering plane in order to minimize the absorption and scatter of hard radiation, which is transmitted through the crystal when white beam is incident. The antitwist mechanism consists of a 1-μm resolution stepper-motor lead-screw drive (not shown), which pushes on the top of the bracket at point C. Because the bracket is spring-loaded in the opposite direction, the mechanism permits adjustment of the crystal twist with respect to the fixed bracket at point B.

Horizontal slits will be used to restrict the beam to within the inner most bending posts because of high strain in the end regions of the crystal. We expect the diffracting length of the crystal will be ≈270 mm, and that, with a symmetrically cut Si(220) crystal, we will obtain a focal spot size of 80-95 μm. The focus size estimate is based on the source demagnification contribution of 10-50 μm (depending on the choice of q) and an anticipated aberration contribution of ≈80 μm, based on the findings of previous work with similar bending schemes.[14,15]

IV. THERMAL MODELING

A two-dimensional finite-element calculation[17] was performed to estimate the temperature distribution in the crystal under white beam operation, where the total power from the source is ≈90 W per horizontal milliradian at 100 mA ring current. The incident flux distribution (in space and energy) was calculated, and, after accounting for absorption in upstream Be windows at 1-BM, we deduced the power distribution absorbed by the crystal. At the monochromator position p = 32 m, the absorbed peak power density for a 1-mm-thick crystal at a typical incidence angle of θ=36° was

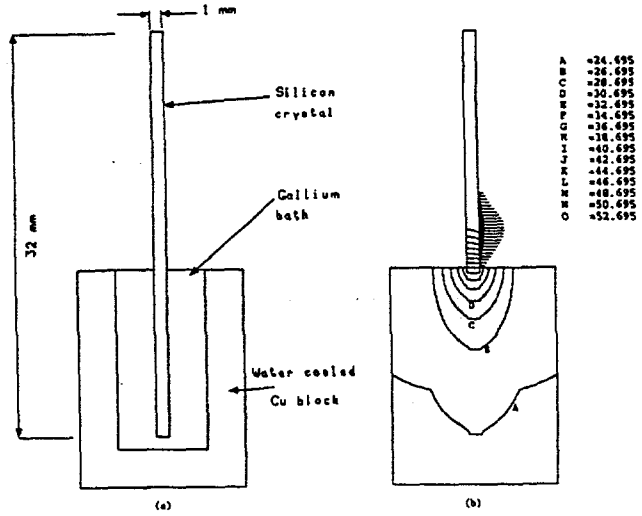

FIG. 3: Finite element thermal model (a) and resulting temperature distribution (b) under white beam illumination. The peak power on the crystal surface is 0.2 W mm^{-2} for an incidence angle of θ=36°. The beam height is 3.6 mm FWHM, centered 3 mm above the top surface of the copper frame and the liquid metal meniscus. The legend on the right identifies the temperature (°C) of each contour. The maximum temperature is ≈37°C above that of the cooling water, which flows along the sides of the copper frame. The maximum temperature difference across the FWHM of the beam at the crystal surface is ≈8°C.

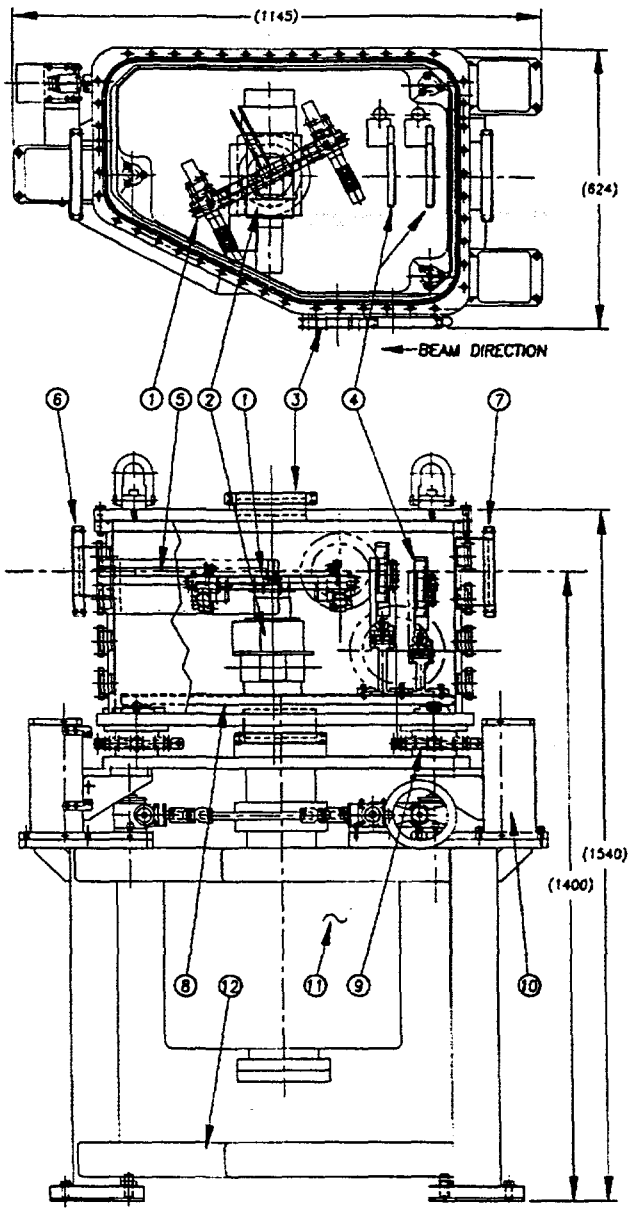

FIG. 4: Sketch of the assembled dispersive monochromator showing the crystal bender (1), motorized crystal motions (2), quartz viewports (3), water-cooled vertical slits (4), exit Be window (5), transmitted beam exit port (6), beam entrance port (7), kinematically mounted base plate (8), kinematic mounts for the vacuum vessel (9), motorized vertical motion (10), ion pump (11) and table frame (12).

found to be 0.2 W mm^{-2} normal to the crystal surface, and the vertical beam size was 3.6 mm FWHM. The power distribution was used as an input to the finite element calculation of the temperature distribution. Thermal conductivities for Si, liquid metal alloy, and Cu were taken to be 1.4, 0.33, and 3.98 $Wcm^{-1}K^{-1}$, respectively. The heat transfer coefficient between the Si and the liquid was 20 $Wcm^{-2}K^{-1}$,[18] and perfect heat transfer was assumed between the liquid and the Cu. Because the device is to operate in vacuum, the only cooling in the calculation was via a heat transfer (0.5 $Wcm^{-2}K^{-1}$) to cooling water at 20°C. The model and resulting equilibrium temperature distribution are shown in Figure 3. Also shown is the distribution of absorbed power in the crystal, which is assumed to be applied at the surface. The maximum temperature is ≈37°C above the coolant temperature and is observed throughout the top half of the crystal. The maximum temperature difference across the FWHM of the beam at the crystal surface is 8°C, which is small enough to prevent significant broadening of the diffraction profile. When an upstream mirror is installed on the beamline, the heat load on the crystal will be reduced by ≈40%, and the maximum temperature and gradient across the beam spot will be reduced accordingly.

V. VACUUM VESSEL

An assembly of the monochromator tank and table is illustrated in Figure 4. The tank contains the crystal bender and both tilt and θ motorized rotation stages, in addition to a horizontal translation stage that can move the crystal entirely out of the beam. The latter permits transmission of the beam to a downstream station. Water-cooled vertical slits define the beam on the crystal. The internal components are all affixed to a kinematically mounted plate inside the vacuum vessel, such that their alignment is protected from vacuum-induced deformations of the vessel. The exit Be window is 406 mm long, permitting operation over an angular range of 2θ=20-85°. The whole vessel is kinematically mounted to a custom table that has 100 mm of vertical travel. An ion pump is expected to maintain the vacuum to 10^{-7} Torr.

ACKNOWLEDGMENTS

We would like to thank K. Finkelstein, D. Mills, G. Navrotski, W. Schildkamp and G. Srajer for their review of the design and K. Gofron for his comments. We also thank J. Barraza, D. Shu, P. Belko, K. Potter and R. Swanson for their technical contributions and S. Picologlou for editing the manuscript. This work was supported by the U.S. Department of Energy, BES-Material Sciences, under Contract No. W-31-109-ENG-38.

[1]R.P. Phizackerley, Z.U. Rek, G.B. Stephenson, S.D. Conradson, K.O. Hodgson, T. Matsushita, H. Oyanagi, J. Appl. Cryst. **16**, 220 (1983).
[2]A.M. Flank, A. Fontaine, A. Jucha, M. Lemonnier, D. Raoux, C. Williams, Nucl. Instrum. Methods **208**, 651 (1983).
[3]H. Tolentino, F. Baudelet, E. Dartyge, A. Fontaine, A. Lena, G. Tourillon, Nucl. Instrum. Methods Phys. Res. **A289**, 307 (1990).
[4]P.G. Allen, S.D. Conradson, J.E. Penner-Hahn, Synchrotron Rad. News **5**, 16 (1992).
[5]M.A. Beno, G.S. Knapp, P. Armond, D.L. Price, M.-L. Saboungi, Rev. Sci. Instrum. **66(2)**, 1308 (1995).
[6]H. Straigier, J.O. Cross, J.J. Rehr, L.B. Sorensen, C.E. Bouldin, J.C. Woicik, Phys. Rev. Letters **69**, 3064 (1992).
[7]P.L. Lee, M.A. Beno, C.M. Ogata, G.S. Knapp, G. Jennings **66(2)**, 1425 (1995).
[8]B. Rodricks, Rev. Sci. Instrum. **66(2)**, 1456 (1995).
[9]Z. Cai, B. Lai, W. Yun, D. Legnini, E. Gluskin, P. Ilinski, ANL, unpublished information, 1995.

[10]T. Matsushita and U. Kaminaga, J. Appl. Cryst. **13**, 465 (1980); T. Matsushita and U. Kaminaga, J. Appl. Cryst. **13**, 472 (1980).
[11]R. Caciuffo, S. Melone, F. Rustichelli, Physics Reports **152**, 1 (1987).
[12]M. Sanchez del Rio, F. Cerrina, Rev. Sci. Instrum. **63**, 936 (1992).
[13]F. D'acapito, F. Boscherini, M. Marcelli, Rev. Sci. Instrum. **63**, 899 (1992).
[14]P. M. DeWolff, in *Selected Topics in X-Ray Crystallography from the Delft Institutes*, edited by J. Bouman (Interscience, New York, 1951), p. 254.
[15]P.G. Allen, S.D. Conradson, J.E. Penner-Hahn, J. Appl. Cryst. **26**, 1723 (1993).
[16]N. Bliss, J. Bordas, B.D. Fell, N.W. Harris, W.I. Helsby, G.R. Mant, W. Smith, E. Towns-Andrews, Rev. Sci. Instrum. **66(2)**, 1311 (1995).
[17]ANSYS Rev. 5.0a, general purpose finite element analysis code, ANSYS Inc., 201 Johnson Rd., Houston, PA USA 15342-1300.
[18]Based on measurements by L. Assoufid on the heat transfer coefficient at the diamond-gallium interface, to appear in this volume.

DISCLAIMER

This report was prepared as an account of work sponsored by an agency of the United States Government. Neither the United States Government nor any agency thereof, nor any of their employees, makes any warranty, express or implied, or assumes any legal liability or responsibility for the accuracy, completeness, or usefulness of any information, apparatus, product, or process disclosed, or represents that its use would not infringe privately owned rights. Reference herein to any specific commercial product, process, or service by trade name, trademark, manufacturer, or otherwise does not necessarily constitute or imply its endorsement, recommendation, or favoring by the United States Government or any agency thereof. The views and opinions of authors expressed herein do not necessarily state or reflect those of the United States Government or any agency thereof.